Local synaptic integration enables ON-OFF asymmetric and layer-specific visual information processing in vGluT3 amacrine cell dendrites

Minggang Chen[a], Seunghoon Lee[a], and Z. Jimmy Zhou[a,b,c,1]

[a]Department of Ophthalmology and Visual Science, Yale School of Medicine, New Haven, CT 06510; [b]Department of Cellular and Molecular Physiology, Yale School of Medicine, New Haven, CT 06510; and [c]Department of Neurobiology, Yale School of Medicine, New Haven, CT 06510

Edited by King-Wai Yau, Johns Hopkins University School of Medicine, Baltimore, MD, and approved August 24, 2017 (received for review June 28, 2017)

A basic scheme of neuronal organization in the mammalian retina is the segregation of ON and OFF pathways in the inner plexiform layer (IPL), where glutamate is released from ON and OFF bipolar cell terminals in separate inner (ON) and outer (OFF) sublayers in response to light intensity increments and decrements, respectively. However, recent studies have found that vGluT3-expressing glutamatergic amacrine cells (GACs) generate ON-OFF somatic responses and release glutamate onto both ON and OFF ganglion cell types, raising the possibility of crossover excitation in violation of the canonical ON-OFF segregation scheme. To test this possibility, we recorded light-evoked Ca^{2+} responses from dendrites of individual GACs infected with GCaMP6s in mouse. Under two-photon imaging, a single GAC generated rectified local dendritic responses, showing ON-dominant responses in ON sublayers and OFF-dominant responses in OFF sublayers. This unexpected ON-OFF segregation within a small-field amacrine cell arose from local synaptic processing, mediated predominantly by synaptic inhibition. Multiple forms of synaptic inhibition compartmentalized the GAC dendritic tree and endowed all dendritic varicosities with a small-center, strong-surround receptive field, which varied in receptive field size and degree of ON-OFF asymmetry with IPL depth. The results reveal a form of short-range dendritic autonomy that enables a small-field, dual-transmitter amacrine cell to process diverse dendritic functions in a stratification level- and postsynaptic target-specific manner, while preserving the fundamental ON-OFF segregation scheme for parallel visual processing and high spatial resolution for small object motion and uniformity detection.

vGluT3 amacrine cell | retinal processing | synaptic integration

In the mammalian retina, ON and OFF bipolar cells release glutamate from their axon terminals in the inner half and the outer half of the inner plexiform layer (IPL), respectively (1–3), except for the rare cases of ectopic, en passant glutamate release from the axonal shaft (4, 5). This anatomically segregated processing of ON and OFF light-evoked excitatory signals serves as a fundamental building block for subsequent image processing in the visual system (6, 7). However, recent studies have found that a small-field, diffusely ramifying amacrine cell type containing the vesicular glutamate transporter 3 (vGluT3) (8–13) releases glutamate (14–16) in addition to a conventional amacrine cell transmitter, glycine (16, 17). This glutamatergic amacrine cell (GAC) is believed to release glutamate from its neurites in both ON and OFF IPL sublayers, because both ON direction-selective and OFF alpha ganglion cells receive glutamatergic input from it (14, 16). Interestingly, patch-clamp recordings from the GAC soma show depolarization to both the onset and the offset of center light stimulation (14, 18, 19). If GACs are electrotonically compact, as is generally believed for small-field amacrine cells (20), a parsimonious prediction would be that GACs release glutamate in both ON and OFF IPL sublayers in response to both center light ON and OFF (14). An ON release of glutamate in the OFF layer or vice versa ("cross-layer" glutamate release) would introduce serious signal contamination between ON and OFF excitatory channels in the IPL and challenge the basic organizational scheme of ON-OFF parallel processing. This paradox motivated us to investigate the basic dendritic physiology of GACs.

In this study, we used two-photon Ca^{2+} imaging from dendrites of individual GACs infected with the genetically encoded Ca^{2+} indicator GCaMP6s (21) to address three questions. First, does glutamate release from GACs violate the ON-OFF segregation scheme in the IPL? Second, can a small-field amacrine cell like GAC support short-range, isolated dendritic processing? Third, if GACs can support local processing, what are the underlying mechanisms and functional consequences? Preliminary results of this study have been reported previously in abstract form (22).

Results

Asymmetric ON-OFF Ca^{2+} Responses from Local Dendritic Regions of GACs. To understand how various parts of a GAC process visual signals, we sparsely infected GACs with GCaMP6s in vGluT3-cre-tdTomato mice (Fig. 1*A*, Fig. S1, and Movie S1). Individual GACs expressing both tdTomato and GCaMP6s in the INL were imaged in the whole-mount retina under a two-photon microscope. These cells ramified mainly between 20% and 60% of the IPL depth, with a minor portion of dendrites found outside of this main band, and showed typically one to two relatively thick primary dendrites that descended from the soma and branched off both radially and laterally into secondary and higher-order dendritic segments, as reported previously (8, 9, 13, 14, 18, 19). The dendritic field was irregularly shaped, with an equivalent field diameter (defined as the diameter of a circle that has the same area as

Significance

Retinal vGluT3 amacrine cells (GACs) release glutamate and glycine to enhance and suppress contrast/motion sensitivity, respectively. GACs' relatively compact size and diffuse ramification pattern suggest global dendritic processing of visual signals across ON and OFF sublayers of the inner plexiform layer. Surprisingly, we find that signal spread in GAC dendrites is limited in both vertical and lateral dimensions. Vertical restriction preserves the fundamental ON-OFF segregation scheme, while lateral restriction enables high-resolution visual processing within a sublayer. Both types of local processing are achieved mainly by synaptic inhibition, though facilitated by intrinsic electrotonic decay. The ability to encode visual signals locally in dendritic segments allows GACs to function in a multiplexed circuit, where the outputs are fine-tuned for diverse, circuit-specific targets.

Author contributions: M.C., S.L., and Z.J.Z. designed research; M.C. and S.L. performed experiments; M.C., S.L., and Z.J.Z. analyzed data; and M.C., S.L., and Z.J.Z. wrote the paper.

The authors declare no conflict of interest.

This article is a PNAS Direct Submission.

See Commentary on page 11268.

[1]To whom correspondence should be addressed. Email: jimmy.zhou@yale.edu.

This article contains supporting information online at www.pnas.org/lookup/suppl/doi:10.1073/pnas.1711622114/-/DCSupplemental.

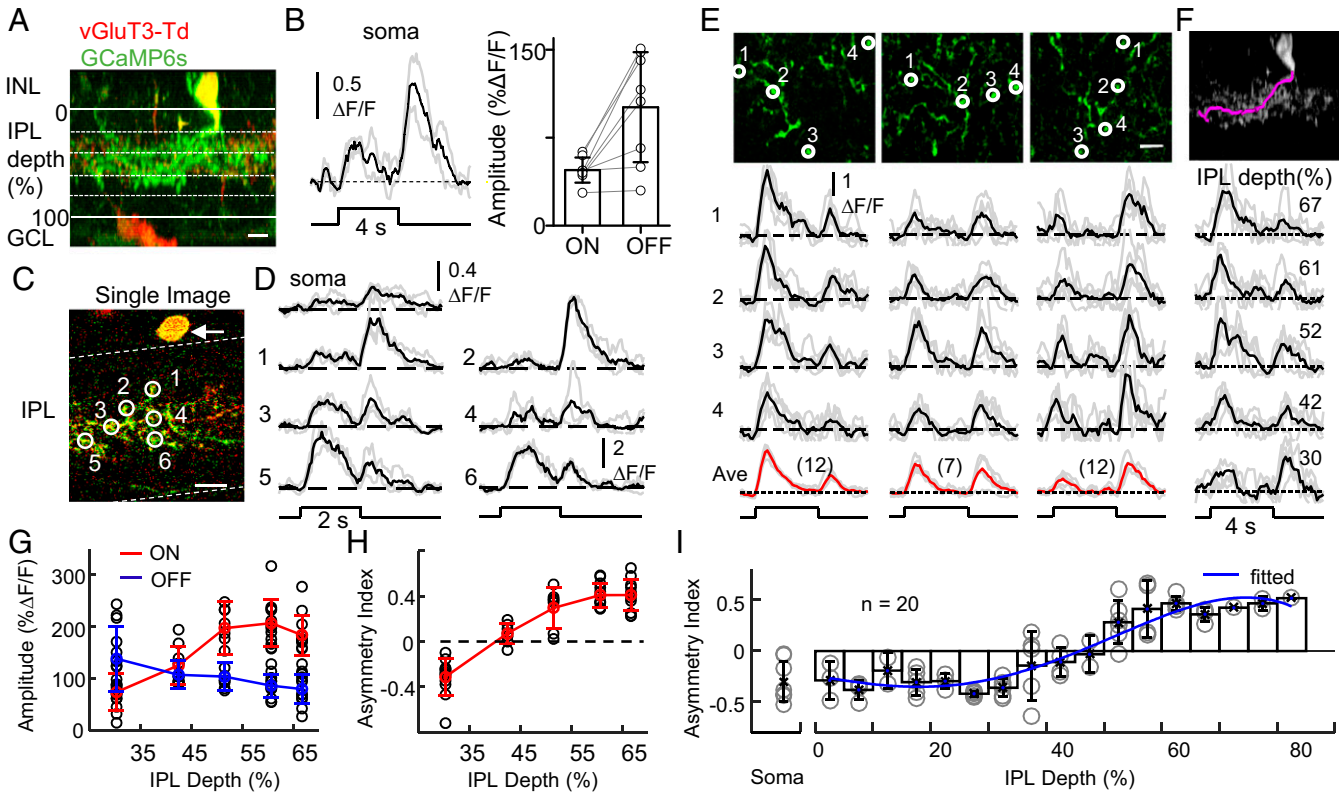

Fig. 1. Layer-dependent asymmetric ON-OFF Ca^{2+} responses from single GACs. (*A*) Cross-sectional reconstruction of a GAC infected with GCaMP6s (green) in a vGluT3-Cre/tdTomato (red) mouse retina. GCL, ganglion cell layer; INL, inner nuclear layer; IPL, inner plexiform layer. (Scale bar: 10 μm.) (*B*, *Left*) An example of somatic Ca^{2+} response to a center spot flash (100 μm diameter); black, averaged response; gray, individual trails. (*B*, *Right*) Mean peak ON and OFF somatic response amplitudes ($n = 8$ cells). (*C*) Image of a GCaMP6-expressing GAC in a titled retinal area, showing the soma (arrow) and dendrites at different IPL depths on a single two-photon focal plane. Dashed lines indicate the IPL boundaries. (Scale bar: 10 μm.) (*D*) Ca^{2+} responses from the cell in *C*, showing IPL depth-dependent asymmetric ON-OFF responses from the soma and six varicosities selected from different IPL depths. (*E*, *Top*) Two-photon images of the cell in *A* in flat-mount, showing (from left to right) dendrites at IPL depths of 61%, 42%, and 30%. (*E*, *Middle*) Ca^{2+} responses from four randomly selected varicosities (black, averaged responses; gray, individual trials). (*E*, *Bottom*) Responses from all analyzed varicosities (number indicated in parentheses) at each of the three IPL depths. Red, averaged responses, gray, individual trials. (*F*, *Top*) Reconstruction of a continuous GAC dendrite coursing through different IPL depths (pink). (*F*, *Bottom*) Responses from varicosities at different IPL depths of the reconstructed dendrite in the top panel, showing changes in ON-OFF asymmetry along the dendrite. (*G*) Peak ON-OFF response amplitudes of varicosities located at different IPL depths of the cell shown in *A*. Black circles, individual varicosities; color circles and error bars, mean and SD, respectively. (*H*) Asymmetry index of varicosities at different IPL depths for the cell in *A*. (*I*) Asymmetry index of dendritic varicosities as a function of IPL depth ($n = 20$ cells) and of soma ($n = 8$ cells). Circles, individual cells; bars and error bars, mean and SD, respectively; blue line, polynomial fit.

the dendritic field) of 87 ± 13 μm and 91 ± 8 μm ($n = 5$ cells; $P = 0.36$) in the ON and the OFF sublamina, respectively (Fig. S1). The entire dendritic tree, except for initial sections of the primary dendrites, was decorated with numerous varicosities, which were often separated by thin dendritic segments (Movie S1).

When stimulated with a center light spot (100 μm diameter), a GAC generated somatic ON-OFF Ca^{2+} responses, showing a smaller ON component and a larger OFF component (Fig. 1*B*), consistent with previously reported patch-clamp results (14, 18, 19). However, when the retina was tilted at an angle with respect to the horizontal plane so that the soma and dendritic segments from different IPL depths could be imaged simultaneously on a single two-photon focal plane, different regions of the GAC dendritic tree exhibited markedly different responses to the same center spot illumination, showing OFF-dominant responses in the outer IPL, ON-OFF responses in the mid IPL, and ON-dominant responses in the inner IPL (Fig. 1 *C* and *D*). Sequential, layer-by-layer imaging of GAC dendrites throughout the IPL depths in horizontally placed flat-mount retinas confirmed the sublayer-specific ON-OFF asymmetry in GAC responses to center light stimulation (Fig. 1*E*). Notably, the differences in response polarity and asymmetry were found not only between dendritic sectors belonging to different primary or secondary dendrites, but also between sectors belonging to different IPL depths of a same continuous dendrite (Fig. 1*F*; $n = 11$ continuous dendrites chosen at random from five cells). As the dendritic ramification depth increased in the IPL, the ON response amplitude increased, whereas the OFF response amplitude decreased (Fig. 1*G*). The ON-OFF response asymmetry index (AI; defined as $[R_{ON} - R_{OFF}]/[R_{ON} + R_{OFF}]$, where R_{ON} and R_{OFF} are ON and OFF response amplitude, respectively) changed monotonically from approximately −0.4 at 30% IPL depth to approximately +0.4 at 70% IPL depth (Fig. 1*H*). A plot of AI (averaged from 20 GACs) as a function of ramification depth revealed a reversal of asymmetry (AI = 0) at ∼45% IPL depth, corresponding to the demarcation between ON and OFF BC axon terminals (Fig. 1*H*). The finding of a sublayer-specific ON-OFF response asymmetry contradicts the previous assumption that narrow-field amacrine cells like GACs have a consistent light response polarity throughout their dendritic trees, as in the case of AII amacrine cells (23, 24) (Fig. S2).

Consistent with the asymmetric Ca^{2+} responses in ON and OFF sublayers, two-photon imaging from GAC dendrites that were selectively infected with the glutamate sensor, iGluSnFR (25), showed no detectable glutamate release from ON dendrites at the offset of center light stimulation, or from OFF dendrites at the onset of center light stimulation, even though glutamate release was detected from these dendrites in response to exogenous application of NMDA ($n = 8$; Fig. S3).

Layer-Specific Receptive-Field Properties of GAC Dendrites. A layer-by-layer analysis of dendritic responses of GACs to light spots of various diameters (25–500 μm) revealed some distinct receptive field properties of local dendrites. First, all dendritic varicosities in both ON and OFF sublayers had a strong inhibitory surround, such that spots larger than 200 μm in diameter nearly completely suppressed the responses (Fig. 2*A*), indicating that the release of glutamate and glycine is activated by local, but not global, stimulation at each release site. Second, as the spot diameter increased, the degree of asymmetry (i.e., absolute value of AI) increased for responses in the ON sublayer, but decreased for responses in the OFF sublayer (Fig. 2 *A* and *B*). Third, although the dendritic field size was similar in the ON and OFF sublayers (Fig. S1), the spatial profile of the response to spot stimulation (averaged from varicosities within a ~50 × 50 μm^2 area) showed a larger receptive field size in the ON sublayer than in the OFF sublayer, with a spot diameter at half-maximum response amplitude ($d_{1/2}$) of 241 ± 36 μm for the ON response and 151 ± 30 μm for the OFF response ($n = 7$ cells; $P < 0.0001$; Fig. 2 *C* and *D*). A difference-of-Gaussian fit of the averaged receptive field profile yielded an excitatory receptive field center with a diameter of ~160 μm for ON responses and ~105 μm for OFF responses, and an inhibitory receptive field surround with a diameter of ~619 μm for ON responses and ~442 μm for OFF responses (*Materials and Methods* and Fig. 2*D*). Thus, differences in presynaptic and postsynaptic inhibition from the surround contributed to the difference in ON and OFF receptive field size, which may in turn explain the increase (or decrease) in the absolute value of the asymmetric index in the ON (or OFF) sublayer with increasing light spot size (Fig. 2*B*). Fourth, while the ON and OFF receptive field center size was different, the spatial profile of the ON response was similar in the ON and OFF sublayers, as was that of the OFF response (Fig. 2*E*), indicating that the small ON response in the OFF dendrites of a GAC originated from the ON dendrites, and vice versa. Indeed, L-AP4, which blocks ON bipolar cell input to the ON sublayer, completely blocked the ON responses from the OFF dendrites of GACs ($n = 4$ cells), whereas ACET, which blocks OFF bipolar input to the OFF sublayer, blocked the OFF response of ON GAC dendrites nearly completely ($n = 4$ cells; Fig. 2*F*), confirming that the ON response originated in the ON sublayer and decayed significantly as it spread to the OFF sublayer, and vice versa for the OFF response.

Synaptic Contributions to the ON-OFF Response Asymmetry of GAC Dendrites. To determine whether the sublayer-specific ON-OFF response asymmetry is shaped predominantly by local synaptic inhibition or by intrinsic electrotonic isolation of the dendrites, we examined the effects of inhibitory synaptic receptor antagonists on the responses of GAC dendrites to center spot (100 μm diameter) and large-field (500 μm diameter) illumination. Blocking $GABA_A$ and $GABA_C$ receptors with SR-95531 (SR; 17 μM) and TPMPA (50 μM) brought out strong responses to large-field illumination in both ON and OFF sublayers, eliminating the characteristically strong surround inhibition of the cell (Fig. 3 *A* and *B*). In the ON sublayer, SR + TPMPA significantly increased the amplitude of the OFF response to the center spot (ΔF/F increase from 85 ± 59% to 207 ± 92%; $P = 0.002$; $n = 5$ cells), but had a much smaller effect on the ON response amplitude (ΔF/F increase from 155% ± 79% to 201 ± 100%; $P = 0.06$; $n = 5$ cells) (Fig. 3 *A* and *C*), resulting in nearly complete elimination of ON-OFF response asymmetry (AI decrease from 0.31 ± 0.12 to −0.03 ± 0.04; $P = 0.003$; $n = 5$ cells) (Fig. 3*E*). In the OFF sublayer, SR + TPMPA increased the ON response amplitude to the center spot (ΔF/F increase from 94 ± 55% to 164 ± 64%; $P = 0.005$; $n = 5$ cells), but did not significantly affect the OFF responses (ΔF/F increase from 259 ± 134% to 281 ± 112%; $P = 0.42$; $n = 5$ cells) (Fig. 3 *B* and *D*), leading to a significant reduction in the degree of response asymmetry (decrease in absolute value of AI from 0.47 ± 0.12 to 0.24 ± 0.08; $P = 0.01$; $n = 5$ cells) (Fig. 3*F*). Thus, GABAergic inhibition played a critical role in shaping the ON-OFF asymmetric responses in GAC dendrites. GABAergic inhibition was also responsible for the strong surround inhibition of both ON and OFF dendrites of GACs.

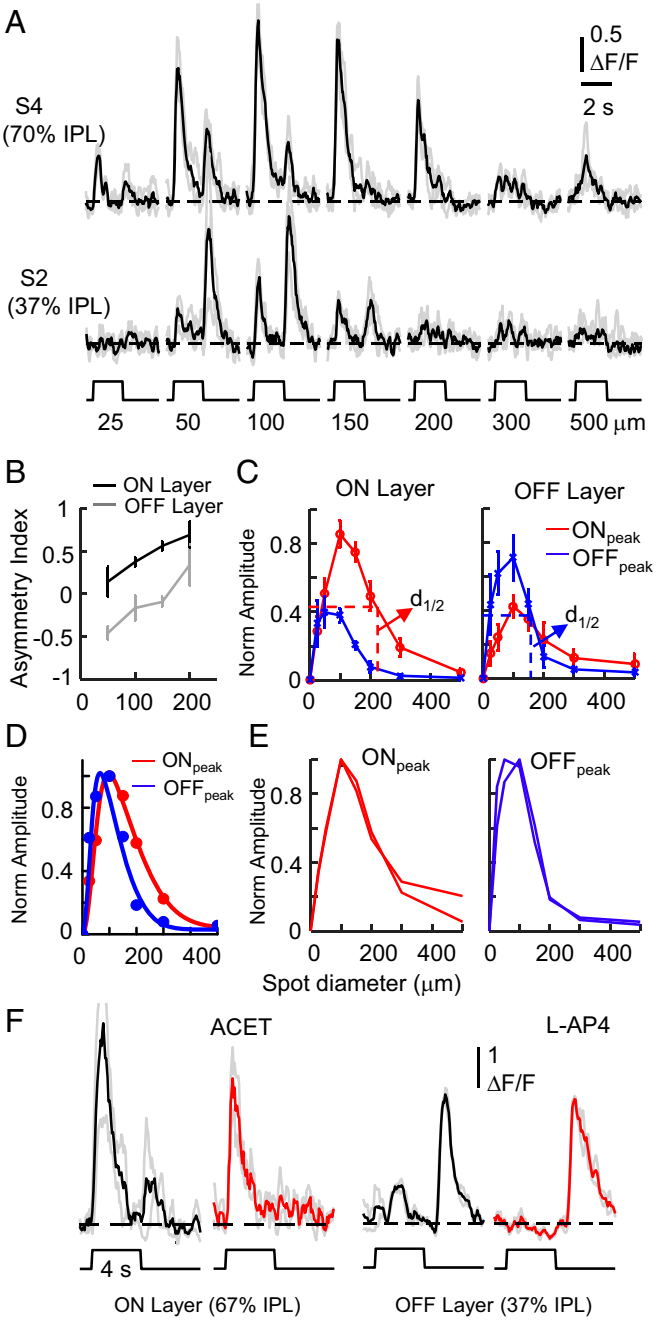

Fig. 2. Receptive field properties of GAC dendrites. (*A*) Averaged Ca^{2+} responses from varicosities in a ~50 × 50 μm^2 area at ON (S4) and OFF (S2) sublayers to light spots of increasing diameters. (*B*) Asymmetry index of ON (black) and OFF dendrites (gray) as a function of spot size. (*C*) Spatial profile of averaged ON (red) and OFF (blue) peak response amplitudes from ON sublayer (*Left*, normalized to the maximum ON peak response amplitude) and OFF sublayer (*Right*, normalized to maximum OFF peak response amplitude). $n = 7$ cells. Error bars represent SEM. (*D*) Spatial profile of normalized average ON response from the ON sublayer (red) and OFF response from the OFF sublayer (blue), fitted by a difference-of-Gaussian model (*Materials and Methods*). (*E*) Overlay of normalized ON response profiles from ON and OFF sublayers (*Left*), and normalized OFF response profiles from ON and OFF sublayers (*Right*). (*F*) Blockade of OFF response in ON sublayers by ACET (10 μM) and ON response in OFF sublayers by L-AP4 (20 μM). For statistical analysis, data from ON and OFF sublayers are pooled from all IPL depths in the ON and OFF sublayers, respectively.

In contrast, blocking glycine receptors with strychnine (1 μM) did not bring out a response to the large-field light stimulation from either ON or OFF dendrites (Fig. 3 *G* and *H*), suggesting that the strong surround inhibition came predominantly from GABAergic amacrine cells (Fig. 3 *A* and *B*). For the center light stimulation, in the ON sublayer, strychnine did not have a consistent, statistically significant effect on the ON response amplitude (ΔF/F: 290 ± 125% to 195 ± 45%; $P = 0.16$; $n = 4$ cells) and reduced the OFF response amplitude only slightly (ΔF/F: 104 ± 30% to 78 ± 22%; $P = 0.08$; $n = 4$ cells), resulting in no statistically significant change in response asymmetry (AI: 0.44 ± 0.18 to 0.43 ± 0.1; $P = 0.79$; $n = 4$ cells) (Fig. 3 *G*, *I*, and *K*), although strychnine seemed to slow the decay of ON responses. However, in the OFF sublayer, strychnine significantly enhanced the amplitude of the ON response to a center spot (ΔF/F: 152 ± 72% to 230 ± 109%; $P = 0.02$; $n = 5$ cells), suggesting a strong glycinergic ON-to-OFF crossover inhibition (Fig. 3 *H* and *J*). Curiously, strychnine also reduced the amplitude of the OFF response to the center spot (ΔF/F: 299 ± 123% to 121 ± 88%; $P = 0.02$; $n = 5$ cells) (Fig. 3 *H* and *J*), resulting in reversal of the polarity of asymmetry (Fig. 3*L*). Suppression of OFF excitatory activity by strychnine has been previously reported for retinal ganglion cells and attributed to a possible enhancement (disinhibition) of GABAergic feedback inhibition of OFF bipolar cells and/or an interference with crossover inhibition of bipolar, amacrine, and ganglion cells (26). These two possibilities might be further tested by sequentially applying SR/TPMPA and strychnine; however, in the presence of all these drugs, GACs generated so much spontaneous baseline activity so as to make light responses no longer distinguishable, precluding such experiments.

Taken together, the foregoing results suggest that the asymmetry in the ON-OFF response of GAC dendrites to center light stimulation was largely a result of synaptic inhibition mediated by a combination of glycinergic and GABAergic interactions. The suppression of signal spread from the ON to OFF dendrites was mediated by both glycinergic and GABAergic inhibition, whereas the suppression of signal spread from the OFF to ON dendrites seemed dominated by GABAergic interactions. In addition, GABAergic, but not glycinergic, interactions played a dominant role in shaping the strong surround inhibition of GAC dendrites in all sublayers (*Discussion*).

Localized Ca^{2+} Responses in GAC Dendritic Branches. To investigate whether dendritic signal processing is also isolated laterally within each IPL sublayer, we used a small light spot (25 μm diameter) to stimulate local dendritic regions and varicosities within the dendritic field of a GAC. Unlike the 100-μm-diameter center spot, which activated nearly all varicosities in each sublayer of GAC dendrites, a small light spot was effective in activating varicosities only in a local

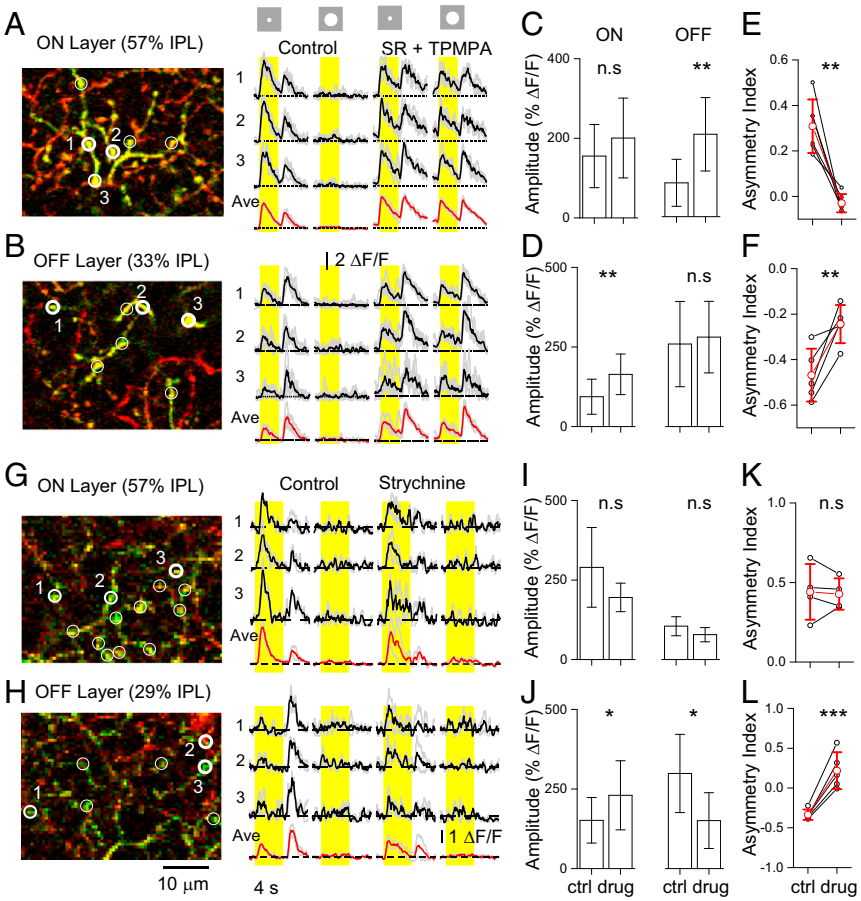

Fig. 3. Role of GABAergic and glycinergic inhibition in asymmetric ON-OFF responses of GAC dendrites. (*A* and *B*) Responses from the ON (*A*) and OFF (*B*) sublayers of a GAC to center (100 μm diameter) and large-field (500 μm diameter) light stimulation in control and in the presence of SR (17 μM) and TPMPA (50 μM). (*C* and *D*) Effects of SR + TPMPA on the peak response amplitude in the ON (*C*) and OFF (*D*) sublayers. (*E* and *F*) Effects of SR + TPMPA on AI in the ON (*E*) and the OFF (*F*) sublayers. (*G* and *H*) Responses from the ON (*G*) and OFF (*H*) sublayers of a GAC to center (100 μm diameter) and large-field (500 μm diameter) light stimulation in control and in the presence of strychnine (1 μM). (*I* and *J*) Effects of strychnine on the peak response amplitude in the ON (*I*) and OFF (*J*) sublayers. (*K* and *L*) Effects of strychnine on the AI in the ON (*K*) and OFF (*L*) sublayers. Black traces, responses from three numbered varicosities; red traces, average responses from all circled varicosities as shown on the left. Error bars represent SD. n.s., not significant ($P > 0.05$); *$P < 0.05$; **$P < 0.01$; ***$P < 0.001$. For statistical analysis, data from ON and OFF sublayers are pooled from all IPL depths in the ON and OFF sublayers, respectively.

region within the vicinity of the stimulus (Fig. 4*A*). Varicosities located at a distance from the stimulus usually gave no clear responses or much smaller responses, indicating that focal excitation was processed locally, with limited lateral spread. Blocking GABAergic inhibition with SR (17 μM) and TPMPA (50 μM) expanded the lateral spread of the response to the small spot stimulation in both ON (n = 2 cells) and OFF (n = 3 cells) sublayers (Fig. 4*B* and Fig. S4). However, strychnine (1 μM) did not have a clear effect on the lateral spread of local responses to small spot stimulation in either ON (n = 3 cells) or OFF sublayer (n = 4 cells), although it significantly enhanced local ON responses in the OFF sublayer (Fig. 4*C* and Fig. S5), in agreement with the results shown in Fig. 3 *H* and *J*. Thus, GABAergic, but not glycinergic, inhibition seemed to play a dominant role in restricting the lateral spread of excitation in GAC dendrites. Notably, even in the presence of SR + TPMPA, there was still a considerable reduction in response amplitude from varicosities distant from the site of local stimulation (Fig. 4*B*), suggesting a possible role of intrinsic electrotonic decay along GAC dendrites as well.

Discussion

Asymmetric ON-OFF Ca^{2+} Responses and Dual Transmitter Releases from Local Dendrites of GACs. Our results demonstrate that GAC dendrites process visual signals locally and generate ON-OFF asymmetric responses in a stratification depth-specific manner. Because GACs release both glutamate and glycine in a Ca^{2+}-dependent manner (14, 16), and because vesicular release probability is a supralinear function of Ca^{2+} concentration (proportional to the third–fourth power of Ca^{2+} concentration; ref. 27), the asymmetric ON-OFF Ca^{2+} signals seen at the varicosities can be expected to lead to more asymmetric ON vs. OFF release probabilities. A rectified release of glutamate from GAC dendrites will effectively avoid crossover excitation, thereby preserving the ON-OFF segregation scheme in the IPL, as supported by the iGluSnFR imaging results (Fig. S3). Similarly, the release of glycine from GAC dendrites is also expected to be segregated between the ON and OFF sublayers, although the degree of rectification may differ between glutamate and glycine releases, depending on the nature of the interactions between local Ca^{2+} dynamics and the release machinery at glutamate and glycine output synapses. Thus, unlike the "prototype" of diffuse, small-field amacrine cells (e.g., the AII amacrine), GACs do not seem to play a major role in glycinergic crossover inhibition, and instead may be involved primarily in local glycinergic inhibition within individual IPL sublayers. Nonetheless, because the precise Ca^{2+} dynamics and the exact Ca^{2+} thresholds for glutamate and glycine releases at the synapses remain unclear, the observation of ON-OFF asymmetric Ca^{2+} responses at GAC varicosities does not exclude the possibility of incomplete ON-OFF segregation of glutamate and/or glycine release at some synapses under certain stimulation conditions. Moreover, our results also suggest that those varicosities exhibiting symmetric ON-OFF Ca^{2+} responses in the middle of the IPL (Fig. 1 *C* and *E*) may have ON-OFF glutamate and/or glycine release, perhaps onto target cells that show ON-OFF light responses, such as uniformity detectors (16, 17).

Synaptic Mechanisms Underlying ON-OFF Asymmetric Responses from Local GAC Dendrites. In contrast to wide-field nonspiking amacrine cells, such as the starburst, which is known to generate local direction-selective response at its distal dendrites (28–31), narrow-field, diffusely stratified amacrine cells are generally believed to be electrotonically compact and to have a uniform response polarity within the cell. Thus, it is surprising to see segregated ON-OFF responses from a GAC dendrite spanning different IPL sublayers, which can be separated by a dendritic distance as short as ~10 μm. Compartmentalized computation within such a short dendritic distance is not likely attributable to pure intrinsic electrotonic isolation. We found that this short-range, intersublayer segregation of dendritic signals was achieved primarily by synaptic inhibition, most likely involving glycinergic/GABAergic ON-to-OFF and GABAergic OFF-to-ON crossover inhibition, and/or local GABAergic and glycinergic inhibitions that suppress the spread of excitation along local

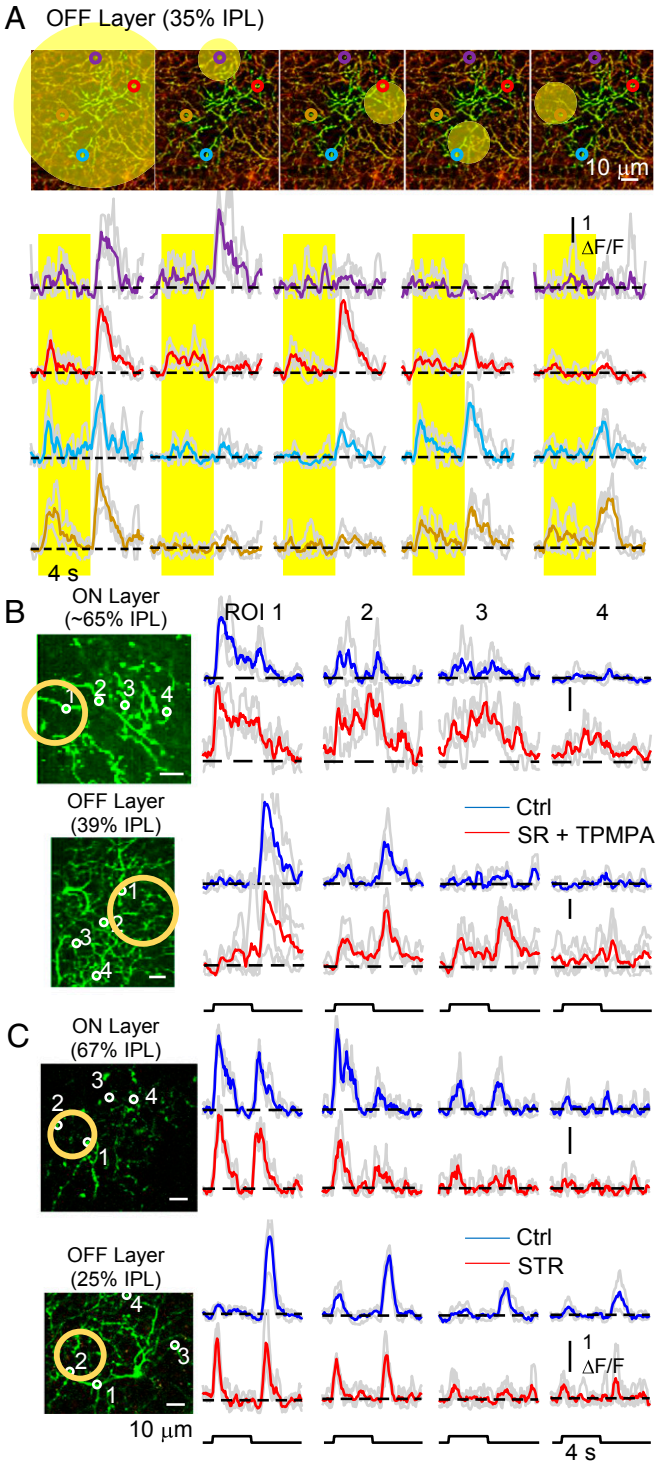

Fig. 4. Local processing of Ca^{2+} signal within GAC dendrites. (*A*) Responses of individual varicosities to a center light spot (*Left*; shaded yellow disk, 100 μm diameter) and a small spot (*Right*; small shaded disk, 25 μm diameter) delivered to four different locations within the dendritic field. Note that the small light spot activated only varicosities near the vicinity of the stimulus, suggesting limited lateral communication among varicosities, and a spatial resolution finer than the dendritic field size. (*B*), SR (17 μM) + TPMPA (50 μM) expanded the lateral spread of the response to small spot illumination within GAC dendrites in both ON and OFF sublayers. (*C*) Strychnine (1 μM) had no clear effect on the lateral spread of Ca^{2+} responses to focal spots within the GAC dendritic field in either ON or OFF sublayers.

dendritic segments (Fig. 3). Other forms of dendritic inhibition, including tonic GABAergic baseline inhibition, also may contribute to the suppression of dendritic signal spread between ON and OFF sublayers by, for example, shunting dendritic segments, while allowing local Ca^{2+} entry through NMDA receptors (Fig. S3).

Receptive Field Structure and Functions of GAC Dendrites. We found that all varicosities in the GAC dendritic tree had a small-center, strong GABAergic-surround receptive field. However, the receptive field size of local dendritic varicosities was larger in the ON layer than in the OFF layer, while the size of the dendritic field was non-statistically significantly different between the ON and OFF layers (Fig. S1), suggesting layer-specific differences in dendritic computation. The ON-OFF asymmetry index also varied with dendritic ramification depth and had a differing dependency on spot size in the ON sublayers and OFF sublayers. In addition to the segregation of dendritic signals between different stratification depths, our results show that signals from varicosities located at the same stratification depth were isolated laterally as well. Individual dendritic varicosities responded differently to a small stimulus spot (25 μm diameter) appearing at different locations within the dendritic field, suggesting that each varicosity had a spatial resolution finer than the dendritic field size. The lateral isolation of signals was dependent largely on GABAergic, but not glycinergic, inhibition and to a lesser degree on electrotonic isolation as well, although the precise underlying mechanism for this remains unclear. Thus, GAC dendrites support local computation in both vertical (radial) and lateral dimensions.

Taken together, our results reveal a previously undescribed form of short-range dendritic autonomy within the relatively small dendritic tree of GAC that enables this diffusely stratified cell to process visual signals locally at different stratification levels where different parts of the dendritic tree interact with different target neurons in a stratification-specific manner. This form of local dendritic processing, together with the dual transmitter system, allows a single GAC to play diverse functional roles in multiple synaptic circuits, while maintaining two binding features of the cell: ON-OFF segregation and a small-center, strong-surround receptive field. The former feature preserves the basic ON-OFF parallel processing scheme in the visual system, and the latter ensures the high spatial resolution and spatial contrast sensitivity essential not only for local/differential object motion detection, but also for uniformity detection and other forms of visual computation in the IPL.

Materials and Methods

All animal procedures were performed in accordance with National Institutes of Health guidelines. We used either vGluT3-Cre mice (19) or vGluT3-tdTomato mice generated by crossbreeding vGluT3-Cre mice with tdTomato mice, strain B6.Cg-*Gt(ROSA)26Sor*$^{tm9(CAG\text{-}tdTomato)Hze}$/J (The Jackson Laboratory). Mouse eyes were injected intravitreally with the virus construct (AAV1 Syn Flex GCaMP6s, WPRE SV40; Penn Vector Core). Single GCaMP6s-expressing GACs were imaged under a two-photon microscope. The light stimulus had an intensity of 3.4×10^{-13} W/μm^2 over a uniform background light of 3.4×10^{-14} W/μm^2 at photoreceptors. The materials and methods used in this study are described in detail in *SI Materials and Methods*.

ACKNOWLEDGMENTS. This work was supported in part by National Institutes of Health Grants EY026065 (to Z.J.Z.) and EY17353 (to Z.J.Z.), an unrestricted grant from Research to Prevent Blindness to Yale Eye Center, and the Marvin L. Sears Professorship at Yale University (to Z.J.Z.).

1. Famiglietti EV, Jr, Kolb H (1976) Structural basis for ON- and OFF-center responses in retinal ganglion cells. *Science* 194:193–195.
2. Famiglietti EV, Jr, Kaneko A, Tachibana M (1977) Neuronal architecture of on and off pathways to ganglion cells in carp retina. *Science* 198:1267–1269.
3. Nelson R, Famiglietti EV, Jr, Kolb H (1978) Intracellular staining reveals different levels of stratification for on- and off-center ganglion cells in cat retina. *J Neurophysiol* 41:472–483.
4. Dumitrescu ON, Pucci FG, Wong KY, Berson DM (2009) Ectopic retinal ON bipolar cell synapses in the OFF inner plexiform layer: Contacts with dopaminergic amacrine cells and melanopsin ganglion cells. *J Comp Neurol* 517:226–244.
5. Hoshi H, Liu WL, Massey SC, Mills SL (2009) ON inputs to the OFF layer: Bipolar cells that break the stratification rules of the retina. *J Neurosci* 29:8875–8883.
6. Euler T, Haverkamp S, Schubert T, Baden T (2014) Retinal bipolar cells: Elementary building blocks of vision. *Nat Rev Neurosci* 15:507–519.
7. Masland RH (2012) The neuronal organization of the retina. *Neuron* 76:266–280.
8. Johnson J, et al. (2004) Vesicular glutamate transporter 3 expression identifies glutamatergic amacrine cells in the rodent retina. *J Comp Neurol* 477:386–398.
9. Haverkamp S, Wässle H (2004) Characterization of an amacrine cell type of the mammalian retina immunoreactive for vesicular glutamate transporter 3. *J Comp Neurol* 468:251–263.
10. Fremeau RT, Jr, et al. (2002) The identification of vesicular glutamate transporter 3 suggests novel modes of signaling by glutamate. *Proc Natl Acad Sci USA* 99:14488–14493.
11. Gong J, et al. (2006) Distribution of vesicular glutamate transporters in rat and human retina. *Brain Res* 1082:73–85.
12. Stella SL, Jr, Li S, Sabatini A, Vila A, Brecha NC (2008) Comparison of the ontogeny of the vesicular glutamate transporter 3 (VGLUT3) with VGLUT1 and VGLUT2 in the rat retina. *Brain Res* 1215:20–29.
13. Marshak DW, et al. (2015) Synaptic connections of amacrine cells containing vesicular glutamate transporter 3 in baboon retinas. *Vis Neurosci* 32:E006.
14. Lee S, et al. (2014) An unconventional glutamatergic circuit in the retina formed by vGluT3 amacrine cells. *Neuron* 84:708–715.
15. Krishnaswamy A, Yamagata M, Duan X, Hong YK, Sanes JR (2015) Sidekick 2 directs formation of a retinal circuit that detects differential motion. *Nature* 524:466–470.
16. Lee S, Zhang Y, Chen M, Zhou ZJ (2016) Segregated glycine-glutamate co-transmission from vGluT3 amacrine cells to contrast-suppressed and contrast-enhanced retinal circuits. *Neuron* 90:27–34.
17. Tien NW, Kim T, Kerschensteiner D (2016) Target-specific glycinergic transmission from VGluT3-expressing amacrine cells shapes suppressive contrast responses in the retina. *Cell Rep* 15:1369–1375.
18. Kim T, Soto F, Kerschensteiner D (2015) An excitatory amacrine cell detects object motion and provides feature-selective input to ganglion cells in the mouse retina. *Elife* 4:e08025.
19. Grimes WN, Seal RP, Oesch N, Edwards RH, Diamond JS (2011) Genetic targeting and physiological features of VGLUT3$^+$ amacrine cells. *Vis Neurosci* 28:381–392.
20. Masland RH (2012) The tasks of amacrine cells. *Vis Neurosci* 29:3–9.
21. Tian L, et al. (2009) Imaging neural activity in worms, flies and mice with improved GCaMP calcium indicators. *Nat Methods* 6:875–881.
22. Lee S, Chen L, Zhou Z (2015) Synaptic properties of vGluT3 amacrine cells in the mouse retina. *Invest Ophthalmol Vis Sci* 56:4377.
23. Borghuis BG, et al. (2011) Imaging light responses of targeted neuron populations in the rodent retina. *J Neurosci* 31:2855–2867.
24. Balakrishnan V, Puthussery T, Kim MH, Taylor WR, von Gersdorff H (2015) Synaptic vesicle exocytosis at the dendritic lobules of an inhibitory interneuron in the mammalian retina. *Neuron* 87:563–575.
25. Marvin JS, et al. (2013) An optimized fluorescent probe for visualizing glutamate neurotransmission. *Nat Methods* 10:162–170.
26. Werblin FS (2010) Six different roles for crossover inhibition in the retina: Correcting the nonlinearities of synaptic transmission. *Vis Neurosci* 27:1–8.
27. Dodge FA, Jr, Rahamimoff R (1967) Co-operative action of calcium ions in transmitter release at the neuromuscular junction. *J Physiol* 193:419–432.
28. Pei Z, et al. (2015) Conditional knock-out of vesicular GABA transporter gene from starburst amacrine cells reveals the contributions of multiple synaptic mechanisms underlying direction selectivity in the retina. *J Neurosci* 35:13219–13232.
29. Lee S, Zhou ZJ (2006) The synaptic mechanism of direction selectivity in distal processes of starburst amacrine cells. *Neuron* 51:787–799.
30. Vlasits AL, et al. (2016) A role for synaptic input distribution in a dendritic computation of motion direction in the retina. *Neuron* 89:1317–1330.
31. Euler T, Detwiler PB, Denk W (2002) Directionally selective calcium signals in dendrites of starburst amacrine cells. *Nature* 418:845–852.
32. Chen M, Lee S, Park SJ, Looger LL, Zhou ZJ (2014) Receptive field properties of bipolar cell axon terminals in direction-selective sublaminas of the mouse retina. *J Neurophysiol* 112:1950–1962.
33. Demb JB, Zaghloul K, Haarsma L, Sterling P (2001) Bipolar cells contribute to nonlinear spatial summation in the brisk-transient (Y) ganglion cell in mammalian retina. *J Neurosci* 21:7447–7454.
34. Rodieck RW (1965) Quantitative analysis of cat retinal ganglion cell response to visual stimuli. *Vision Res* 5:583–601.